

THE ORIGIN OF GAMMA RAYS FROM GLOBULAR CLUSTERS

K. S. CHENG¹, D. O. CHERNYSHOV², V. A. DOGIEL³, C. Y. HUI⁴, AND A. K. H. KONG⁵

¹ Department of Physics, University of Hong Kong, Pokfulam Road, Hong Kong

² Moscow Institute of Physics and Technology, Institutskii lane, 141700 Moscow Region, Dolgoprudnii, Russia

³ I. E. Tamm Theoretical Physics Division of P. N. Lebedev Institute, Leninskii pr, 53, 119991 Moscow, Russia

⁴ Department of Astronomy and Space Science, Chungnam National University, Daejeon, South Korea

⁵ Institute of Astronomy and Department of Physics, National Tsing Hua University, Hsinchu, Taiwan

Received 2010 March 30; accepted 2010 September 7; published 2010 October 20

ABSTRACT

Fermi has detected gamma-ray emission from eight globular clusters (GCs). It is commonly believed that the energy sources of these gamma rays are millisecond pulsars (MSPs) inside GCs. Also it has been standard to explain the spectra of most *Fermi* Large Area Telescope pulsars including MSPs resulting from the curvature radiation (CR) of relativistic electrons/positrons inside the pulsar magnetosphere. Therefore, gamma rays from GCs are expected to be the collection of CR from all MSPs inside the clusters. However, the angular resolution is not high enough to pinpoint the nature of the emission. In this paper, we calculate the gamma rays produced by the inverse Compton (IC) scattering between relativistic electrons/positrons in the pulsar wind of MSPs in the GCs and background soft photons including cosmic microwave/relic photons, background star lights in the clusters, the galactic infrared photons, and the galactic star lights. We show that the gamma-ray spectrum from 47 Tucanae can be explained equally well by upward scattering of either the relic photons, the galactic infrared photons, or the galactic star lights, whereas the gamma-ray spectra from the other seven GCs are best fitted by the upward scattering of either the galactic infrared photons or the galactic star lights. We also find that the observed gamma-ray luminosity is correlated better with the combined factor of the encounter rate and the background soft photon energy density. Therefore, the IC scattering may also contribute to the observed gamma-ray emission from GCs detected by *Fermi* in addition to the standard CR process. Furthermore, we find that the emission region of high-energy photons from GCs produced by the IC scattering is substantially larger than the cores of GCs with a radius >10 pc. The diffuse radio and X-rays emitted from GCs can also be produced by the synchrotron radiation and IC scattering, respectively. We suggest that future observations including radio, X-rays, and gamma rays with energy higher than 10 GeV and better angular resolution can provide better constraints for the models.

Key words: gamma rays: stars – globular clusters: general – globular clusters: individual (47 Tuc, Terzan 5) – pulsars: general

1. INTRODUCTION

Globular clusters (GCs) are the most dense stellar systems, which results in frequent dynamical interactions. In particular, the formation rate per unit mass of low-mass X-ray binaries (LMXBs) is orders of magnitude higher in GCs than in the Galactic field (Katz 1975; Clark 1975). It is generally believed that LMXBs are progenitors of millisecond pulsars (MSPs; e.g., Alpar et al. 1982). Therefore, it is not surprising that 80% of the detected MSPs are located in GCs. So far, 140 MSPs have been detected in 26 GCs.⁶

With the launch of the *Fermi Gamma-ray Space Telescope*, we have entered a new era of high-energy astrophysics. As the sensitivity of the Large Area Telescope (LAT) on the spacecraft is much higher than that of EGRET, it has already led to many interesting discoveries, including the detection of GeV gamma rays from GCs. Shortly after the detection of two GCs with GeV gamma-ray emission, 47 Tucanae (47 Tuc; Abdo et al. 2009) and Terzan 5 (Kong et al. 2010), six other GCs have been identified as gamma-ray emitters (cf. Abdo et al. 2010a, 2010b).

It is generally believed that the gamma-ray emission from GCs either comes from magnetospheres of MSPs or is produced by the inverse Compton (IC) scattering between electrons accelerated in the relativistic pulsar wind and background soft photons. In fact, before the detection of gamma rays from GCs,

Wang et al. (2005) showed that the curvature radiation (CR) spectrum calculated from the outer gap model of Zhang & Cheng (1997) produced from unresolved MSPs in the galactic center can result in a simple power law with an exponential cutoff energy at ~ 3 GeV. They used the observed distribution functions of MSPs from the field, from the GCs, and the combination of these two distributions, and they found that the model spectrum was quite consistent with the diffuse gamma-ray spectrum detected by EGRET in the direction of the galactic center. However, it is important to note that the total gamma-ray spectra calculated from these three different distributions (see Figure 4 of Wang et al. 2005) are actually very similar. Therefore, it is very difficult to constrain the models by using an average spectrum. Recently, Venter & de Jager (2008) and Venter et al. (2009) calculated the expected flux of gamma rays produced by the CR of electrons in pulsar magnetospheres. Venter & de Jager (2008) first calculated the expected GeV flux from 47 Tuc by using an unscreened (pair-starved polar cap) electric field (see, e.g., Harding et al. 2005) for 12 out of the 13 MSPs they considered, and the screened field for only 1 MSP with a relatively high spin-down power based on the approximation of a screened electric field by Dyks & Rudak (2000). Venter et al. (2009) extended the model to include the IC component, which can produce TeV photons. Their model predictions are consistent with the later reported results by *Fermi* (Abdo et al. 2009) but the predicted TeV flux seems to be higher than the observed upper limits for

⁶ <http://www2.naic.edu/~pfreire/GCpsr.html>

47 Tuc (Aharonian et al. 2009). On the other hand, the total number of MSPs is unclear and it is still possible that by adjusting the model parameters both GeV and TeV observed results can be explained in this model.

However, the radio and X-ray properties of MSPs in GCs are found to be rather different from those located in the Galactic field (Bogdanov et al. 2006; Hui et al. 2009a, 2010a). The difference can possibly be related to the complicated multipole magnetic field structure of the MSPs in a cluster, which is a consequence of frequent stellar interaction (cf. Cheng & Taam 2003, and see Section 2 for a more detailed account). In fact, the complicated surface magnetic field structure can have a very dramatic effect on both polar gap and outer gap structures. If the surface local magnetic field of MSPs is of the order of 10^{12} G as suggested by Ruderman (1991), Cheng & Zhang (1999) showed that the polar gap potential drop can reduce to 10^{11} V, which makes GeV-photon production very difficult, whereas a large number of pairs can still be produced via the magnetic pair-creation process. Another consequence of a complicated surface magnetic field is to turn off the outer gap. Ruderman & Cheng (1988) argue that if the open field lines are curving upward due to the effect of local field then, in this case, the electron/positron pair production and outflow can occur on all open field lines. Consequently, the outer magnetospheric gap is quenched by these pairs. Furthermore, Cheng & Taam (2003) have also pointed out that most X-ray spectra of pulsars in 47 Tuc can be described by a thermal spectrum with a characteristic temperature insensitive to the pulsar parameters resulting from the fact that the surface magnetic field structure of MSPs in GCs should be dominated by the complicated multiple field structure, and consequently the polar gap is substantially suppressed and the outer gap should not exist. We also explain why the X-ray luminosity of MSPs in the GCs and MSPs in the field obey different relations with the spin-down power. Zavlin (2006) and Bogdanov et al. (2006) both conclude that the spectral properties of the MSPs in the field and in GCs are found to be different. We have found good reasons to believe that properties of MSPs in GCs differ from MSPs in the field. It should be noted that the spectra of almost all the *Fermi*-LAT pulsars including MSPs, except very young pulsars like the Crab pulsar, can be explained in terms of a CR mechanism. Other models can fit the *Fermi* data of GCs equally well but they cannot be accepted as alternative models unless they have other new predictions and are supported by observations. Nevertheless, with all these observational hints, we propose that there may be an alternative/additional emission mechanism to produce the observed gamma rays detected by *Fermi*-LAT and explore the new predictions from this model.

Bednarek & Sitarek (2007) analyzed gamma-ray emission of electrons accelerated at shock waves originated in collisions of the pulsar winds and/or inside the pulsar magnetospheres when gamma rays are generated by the IC scattering of ultra-relativistic electrons of relic and stellar photons. Both of these models can provide reasonable explanations for the gamma-ray emission from 47 Tuc. It should be noted that both of these models predict that gamma rays are emitted from the core region of GC, i.e., <1 pc, where most MSPs are located. The key difference between these two classes of models is that the IC model predicts the existence of very high energy gamma rays, which can be detected by MAGIC and H.E.S.S.

In this paper, we also study the IC scattering between the relativistic electrons/positrons in the pulsar wind and the background soft photons. We adopt the pulsar wind model proposed by Cheng et al. (2004, 2006). To generalize the soft

photon field in our investigation, in addition to relic photons and the star-light photons in the GC, we include the background soft photons from the galactic disk including the infrared photons and star-light photons of the galactic disk. Our calculations do not restrict the IC scattering only in the core; instead, we extend our calculation to several hundred parsecs from the core of GC. By fitting the observed data of 47 Tuc and Terzan 5, our conclusion is significantly different from the previous findings. This paper is organized as follows. In Section 2, we summarize the observations of 47 Tuc and Terzan 5. In Section 3, we describe the pulsar wind model by Cheng et al. (2004, 2006). In Section 4, we present the spatial dependent IC scattering model. In Section 5, we apply our model to explain the data of 47 Tuc, Terzan 5, and the other six GCs observed by *Fermi*. In Section 6, we discuss how other energy bands can constrain various IC models. We summarize our model predictions including a simple correlation analysis between gamma-ray luminosity and the background soft photon density in Section 7.

2. OBSERVATIONAL PROPERTIES OF γ -RAY EMITTING GCS

2.1. 47 Tuc

Apart from the high collision frequency due to the high stellar density inside the cluster, the relatively high metal content in 47 Tuc can further facilitate the formation of binaries with more efficient magnetic braking (cf. Ivanova 2006). Therefore, a large binary population is expected in 47 Tuc.

With a deep X-ray survey by *Chandra* Observatory, 300 X-ray sources within its half-mass radius have been revealed from 47 Tuc (Heinke et al. 2005). This population contains various classes of exotic binaries, including cataclysmic variables (CVs), chromospherically active binaries (ABs), and LMXBs, as well as MSPs. On the other hand, dedicated radio survey has so far uncovered 23 MSPs in this cluster (Camilo et al. 2000) which have reached a detection threshold of ~ 0.5 mJy kpc². Among these 23 MSPs, 19 have had their X-ray counterparts identified (Bogdanov et al. 2006).

The X-ray luminosities of the 47 Tuc pulsars are in the range of $L_X \sim 10^{30} - 10^{31}$ erg s⁻¹ (Bogdanov et al. 2006). The X-ray spectra of the majority of these pulsars can be well described by a thermal model (blackbody or neutron star hydrogen atmosphere model) with the temperature $T_{\text{eff}} \sim (1-3) \times 10^6$ K and the emission radius $R_{\text{eff}} \sim 0.1-3$ km (Bogdanov et al. 2006). These properties are found to be very different from the MSPs in the Galactic field (see Hui et al. 2009b, and references therein). While the MSPs in 47 Tuc are essentially thermal emitters (except for some that have intrabinary shock observed such as 47 Tuc W), the MSPs in the Galactic field generally require two components to model their X-ray spectra which include a hot polar cap component plus a non-thermal power-law tail (Zavlin 2006).

To account for the differences between the 47 Tuc MSPs (or the MSPs in GCs generally) and the MSP population in the Galactic field, it has been suggested that the absence of non-thermal X-ray from the cluster MSPs can possibly be related to the complicated multipole magnetic field structure (cf. Grindlay et al. 2002; Cheng & Taam 2003). Because of frequent stellar interaction, MSPs in a GC can possibly change their companion several times throughout their lives. As the orientation of the binary after each exchange can differ, the direction of the angular momentum accreted during the mass-transfer phase

subsequent to each exchange can vary, possibly affecting the magnetic field configuration at the neutron star surface. Such an evolution could lead to a much more complicated multipole magnetic field structure for the MSPs in the GCs than in the case of the Galactic field. In such a complicated magnetic field, Ruderman & Cheng (1988) have argued that high-energy curvature photons will be emitted and subsequently converted into pairs to quench the accelerating region. This provides an explanation for the absence of non-thermal emission in the cluster MSPs. For the same reason, the complicated multipole magnetic field structure can also possibly alter the coherent radio emission and provide the explanation for the different radio luminosity distribution of the cluster MSPs in comparison with that of the disk MSP population (Hui et al. 2010a).

Apart from the magnetospheric emission, it has long been speculated that pulsar wind nebulae (PWNe) from the MSPs can have a possible contribution in a GC. In 47 Tuc, the low dispersion measure for its MSP population (Freire et al. 2001) suggests that some mechanism operates to reduce the mass of gas in the central region expected to be accumulated in the $\sim 10^7$ – 10^8 years interval between passages of the cluster through the Galactic disk (cf. Camilo & Rasio 2005). The outflow accompanying the relativistic winds from the MSPs in the cluster could possibly reduce the amount of intracluster gas (cf. Spiegel 1991). Motivated by this insight, Hui et al. (2009a) have systematically searched for the X-ray signature of PWNe within the cores of a group of GCs. However, there is no compelling evidence for any nebular emission that can be found in the cluster cores. In contrast, some MSPs in the field have already been found to associate with PWNe, e.g., Hui & Becker (2006) and Stappers et al. (2003). This non-detection has further suggested that the emission properties of the MSP population in GCs are intrinsically different from those of the MSP in the Galactic field.

Gamma-ray observations can provide us important information for further investigating the differences between these two populations. Shortly after LAT began operating, the gamma-ray emission (>200 MeV) from 47 Tuc was detected, the first time that a GC was detected in this high-energy regime (Abdo et al. 2009). The gamma-ray photons from 47 Tuc are presumably the collective contribution by its MSP population. Its gamma-ray spectrum can be well fitted by an exponentially cutoff power-law model with a photon index of $\Gamma = 1.3 \pm 0.3$ and a cutoff energy of $E_c = 2.5^{+1.6}_{-0.8}$ GeV (Abdo et al. 2009). The energy flux in 0.1–10 GeV is found to be 2.5×10^{-11} erg cm $^{-2}$ s $^{-1}$ (Abdo et al. 2009). For a distance of ~ 4 kpc, the gamma-ray luminosity has put an upper bound for the MSP population in 47 Tuc of 60 (Abdo et al. 2009).

2.2. Terzan 5

Terzan 5 holds the largest MSP population among all the MSP-hosting GCs. Currently, there are 33 pulsars that have been found in Terzan 5 (see Ransom et al. 2005; Hessels et al. 2006). It has been shown that the two-body encounter rate plays an important role in the formation of LMXBs in GCs (Verbunt & Hut 1987; Verbunt et al. 1989). Since both the collision frequency and the metallicity of Terzan 5 are even higher than the values found in 47 Tuc, a larger binary content is expected in Terzan 5. Furthermore, Fruchter & Goss (1990, 2000) have identified strong diffuse radio emission from Terzan 5. By using standard pulsar luminosity function, they estimate that there are 50 MSPs which beam toward Earth and imply 500–2000 MSPs in this GC. By using the cumulative radio luminosity distribution

function, Hui et al. (2010a) have recently predicted that the MSP population in Terzan 5 can be ~ 4 – 5 times higher than that in 47 Tuc. Because of the large number of MSPs, it is expected to have strong γ -ray emission. With data obtained in ~ 17 months of continuous observation by LAT, the expected γ -ray emission from Terzan 5 was eventually detected at a significance level of $\sim 27\sigma$ (Kong et al. 2010). The energy spectrum of Terzan 5 is best described by an exponential cutoff power-law model, with a photon index of 1.9 ± 0.2 and a cutoff energy at 3.8 ± 1.2 GeV. The energy flux in 0.5–20 GeV is found to be $(6.8 \pm 2.0) \times 10^{-11}$ erg cm $^{-2}$ s $^{-1}$. For comparison with the result reported for 47 Tuc, the flux in 0.1–10 GeV is $\sim 1.2 \times 10^{-10}$ erg cm $^{-2}$ s $^{-1}$.

The large reservoir of MSPs in Terzan 5 could also provide the seed electrons for the IC scattering of star-light photons or non-thermal bremsstrahlung emission from the deflection of the electrons by interstellar medium. Recently, *Chandra* observation of Terzan 5 reveals extended diffuse X-ray emission outside the half-mass radius of the cluster. The diffuse emission can be described by a steep power law with a photon index of 0.9 (1–7 keV) and is likely to be non-thermal in origin (Eger et al. 2010).

Comparing the gamma-ray properties of 47 Tuc with those of a recently discovered gamma-ray emitting GC Terzan 5 (Kong et al. 2010), we found that there are certain dissimilarities between these two GCs. First, despite the fact that it has been suggested that Terzan 5 locates at a further distance than 47 Tuc, the gamma-ray flux observed from Terzan 5 is ~ 5 times higher than that of 47 Tuc. Assuming the distance to Terzan 5 is ~ 6 kpc (Kong et al. 2010), instead of 10 kpc, and the distance to 47 Tuc is 4 kpc, implies that the gamma-ray luminosity of Terzan 5 is ~ 12 times of 47 Tuc. If the properties of MSPs in these two clusters are similar and the radiation mechanism is CR, it implies that the number of MSPs in Terzan 5 is 12 times that of 47 Tuc. The observed ratio of MSPs is only ~ 1.5 , so this required ratio seems to be unlikely. On the other hand, if the radiation mechanism is IC of the background soft photons, then the energy density of background photons is another factor to affect the gamma-ray luminosity. According to Strong & Moskalenko (1998), the soft photon densities in Terzan 5 are a factor of ~ 7 in optical and a factor of ~ 5 in infrared higher than that of 47 Tuc. Instead of a factor of 12, the IC model only requires Terzan 5 has ~ 5 times more MSPs than that of 47 Tuc, which is consistent with the prediction by Hui et al. (2010a). Second, the gamma-ray spectrum of 47 Tuc is found to be flatter than that of Terzan 5, $\Gamma = 1.9 \pm 0.2$ (Kong et al. 2010). Third, there is an indication of an excess of γ rays with energies >10 GeV in Terzan 5 with a detection significance of 3.7σ (see Figure 1 in Kong et al. 2010). In the case of 47 Tuc, there is no hint of any excess. These spectral differences may not be easily explained in terms of a simple CR radiation process whereas the IC model, which also depends on an external factor, i.e., the background soft photon energy density, is more flexible for explaining various spectral features.

3. PULSAR WIND MODEL

Rees & Gunn (1974) proposed a theoretical description of interaction between a pulsar and its nebula. They suggested that the central pulsar can generate a highly relativistic particle-dominated wind that passes through the medium in the supernova remnant, forming a shock front. The electrons and positrons in the shock are envisioned to be accelerated to a power-law energy distribution and to synchrotron radiation in the downstream region. However, it is unlikely that electrons/

positrons can carry away all the spin-down power of pulsars near the light cylinder. Kennel & Coroniti (1984) have introduced a magnetization parameter, $\sigma = \frac{B^2}{4\pi n\gamma_w m c^2}$, where B is the magnetic field, n is the particle number density, γ_w is the Lorentz factor of relativistic particles in the wind, and m is the particle mass. In order to explain the observed radiation properties in the Crab nebula, $\sigma \sim 0.003$. e^\pm pairs are produced inside the light cylinder in the polar gap (e.g., Ruderman & Sutherland 1975; Fawley et al. 1977) and/or outer gap (e.g., Cheng et al. 1986). When electrons/positrons leave the light cylinder, they can only carry a very small fraction of spin-down power, which implies $\sigma \gg 1$. Therefore, the magnetization parameter of pulsar wind must evolve from high- σ to low- σ in the downstream. Coroniti (1990) has shown that the pulsar spin-down power initially carried away by low-frequency electromagnetic waves can be converted into particle kinetic energy via the magnetic reconnection process before reaching the shock radius.

Cheng et al. (2004, 2006) studied the non-pulsed X-ray emission of rotation-powered pulsars and found that the non-pulsed X-ray luminosity (L_x^{npul}) is proportional to the pulsar spin-down power (L_{sd}) as $L_x^{\text{npul}} \propto L_{\text{sd}}^{1.4 \pm 0.1}$. They argued that the non-pulsed X-rays should be emitted by the pulsar wind in the shock radius via synchrotron radiation. They used the simple one-zone model developed by Chevalier (2000) to estimate the relation between the spin-down power and the non-pulsed X-ray luminosity. They assumed that if most of the spin-down power is eventually converted into the kinetic energy of protons and the proton current equals the Goldreich-Julian current, \dot{N}_{GJ} (Goldreich & Julian 1969), then the Lorentz factor γ_w of the pulsar wind before it reaches the shock region can be expressed as

$$\gamma_w = 2 \times 10^5 L_{34}^{1/2}, \quad (1)$$

where L_{34} is the spin-down power in units of $10^{34} \text{ erg s}^{-1}$ (Cheng et al. 2004, 2006). With this simple estimation they obtained $L_x^{\text{npul}} \propto L_{\text{sd}}^{p/2}$, where p is the power-law index of electron/positron in the shock region. In general, the pulsar wind should consist of protons and e^\pm pairs. Assuming that the pulsar spin-down power is still carried away by particle kinetic energy, i.e.,

$$L_{\text{sd}} = \gamma_w \dot{N}_{\text{GJ}} m_p c^2 f_{e^\pm}, \quad (2)$$

where we assume that the positive and negative charges are moving with the same speed, m_p is the proton mass, $f_{e^\pm} = 1 + \frac{m_e \eta_{e^\pm}}{m_p}$, and $\eta_{e^\pm} = \frac{\dot{N}_{e^\pm}}{\dot{N}_p}$ is the number ratio between e^\pm pairs and protons. By taking e^\pm pairs into account, the Lorentz factor of the pulsar wind becomes

$$\gamma_w = 2 \times 10^5 f_{e^\pm}^{-1} L_{34}^{1/2}. \quad (3)$$

The value of η_{e^\pm} is model dependent. In the polar gap model, $\eta_{e^\pm} \sim 10^2$ (e.g., Ruderman & Sutherland 1975) which gives $f_{e^\pm} \sim 1$. On the other hand, in the outer gap model the ratio η_{e^\pm} is easily larger than m_p/m_e (e.g., Cheng et al. 1986; Cheng & Zhang 1999). However, the exact value of this ratio also depends on the details of the different outer gap models. For example, Wang et al. (2006), based on the MSP outer gap model proposed by Zhang & Cheng (2003), estimate the rate of electron/positron pairs produced by an MSP with $B = 3 \times 10^8 \text{ G}$ and $P = 3 \text{ ms}$ to be approximately equal to $5 \times 10^{37} e^\pm \text{ s}^{-1}$, which gives $f_{e^\pm} \sim 30$. However, they have assumed that all pairs produced near the neutron surface, which are moving inward initially, can be reflected by the magnetic mirroring effect, and escape through

the open field lines; therefore, their estimate should be an upper limit. Although the exact value of f_{e^\pm} depends on the model details, in general it should be roughly $\sim 1-10$. The fraction of the spin-down power carried away by e^\pm pairs is given by

$$L_{e^\pm} = \frac{f_{e^\pm} - 1}{f_{e^\pm}} L_{\text{sd}} = \zeta_{e^\pm} L_{\text{sd}}. \quad (4)$$

Therefore, the efficiency of the spin-down power ζ_{e^\pm} carried away by pairs is roughly between 0.1 and 1. As suggested by Cheng & Taam (2003), an outer gap may not exist for some MSPs with a complicated surface magnetic field in GCs; if this is true then $\zeta_{e^\pm} \sim 0.1$ for those MSPs without an outer gap. We would like to emphasize again that even if an outer gap does not exist, large numbers of pairs can still be produced by the polar gap. In the Ruderman & Sutherland model, the pair multiplicity is typically $\sim 10^2$. Therefore, in general, the number of pairs is still much higher than the number of protons.

It is interesting to ask how much pulsar wind energy will be lost in the shock region. In the case of the Crab nebula, most of the spin down of pulsars is radiated within the nebula region. However, the unpulsed X-ray luminosity of pulsars, which is assumed to be emitted from the shock region, is only a small fraction of the spin-down power. Furthermore, Hui et al. (2009a) have tried to identify the diffuse X-rays of GCs resulting from pulsar wind shock regions and conclude that there is no evidence that the diffuse X-rays can result from pulsar wind shock regions. They argue that the formation of shock regions in the GCs may be very difficult because the characteristic shock radius is much larger than the characteristic separation of stars due to the very low number density in the GCs. In this paper, we shall assume that pairs can be accelerated by absorbing the low-frequency electromagnetic wave energy produced by the dipole radiation of pulsars to a relativistic speed. If indeed the shock does not exist or is very weak, pairs emitted and accelerated by pulsars can be treated as monoenergetic particles with a Lorentz factor given by Equation (3). Since the particle energy loss in the shock is negligible, the pulsar spin-down power carried away by the pairs is given by Equation (4). However, it is important to note that when pairs diffuse away from the GCs, they suffer the IC energy loss by scattering with the background soft photons. Hence a simple power law with the energy index $\Gamma_e \sim 2$ would be developed at a distance when the diffuse time equals the cooling time (Blumenthal & Gould 1970).

4. INVERSE COMPTON MODEL

One of the main differences between the CR and IC models is the size of the emitting region. The CR of pulsars is emitted from the central region of the GC whose radius is about several parsecs. Such a tiny region cannot be resolved by gamma-ray telescopes and, therefore, it is observed in the gamma-ray range as a point-like source. On the other hand, electrons/positrons ejected by pulsars may fill an extended region around GCs and their IC radiation is observed in this case as an extended source. In this case, we should calculate the spectrum and spatial distribution of electrons/positrons around the GC in order to estimate the IC component of gamma rays.

As usual, cosmic-ray propagation in the interstellar medium is described as a diffusion process (see for details, e.g., Berezhinskii et al. 1990). The equations for the distribution function of electrons $f(\mathbf{r}, E)$ has a standard form

$$\frac{\partial f}{\partial t} - \nabla(D(r)\nabla f) + \frac{\partial}{\partial E} \left(\frac{dE}{dt} f \right) = Q(E, \mathbf{r}, t), \quad (5)$$

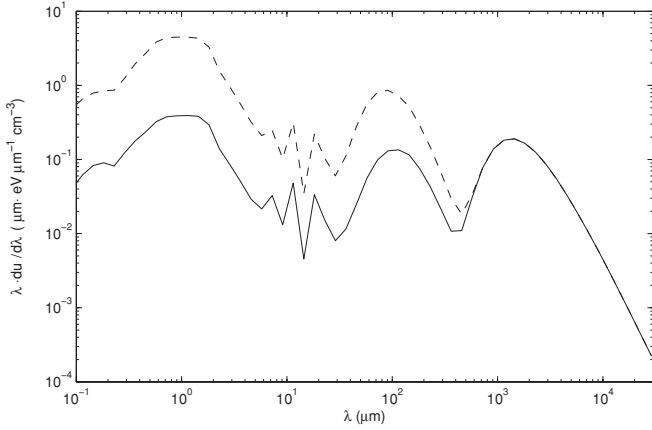


Figure 1. Spectrum of background photons at 47 Tuc (solid line) and Terzan 5 (dashed line).

where $dE/dt \equiv b(E, r)$ is the rate of electron energy losses, $D(r)$ is the coefficient of spatial diffusion, and the function Q describes the injection spectrum and spatial distribution of sources.

Relativistic electrons lose their energy by interacting with the interstellar magnetic field (synchrotron losses) and with background photons (IC losses). The strength of magnetic field in the interstellar medium is about $3 \mu\text{G}$. There are three components of background photons in the Galaxy which interact with electrons: they are relic, infrared, and optical photons. In Figure 1, we present the spectra of background photons at the position of 47 Tuc and Terzan 5 in the Galaxy which were obtained with the GALPROP code (Strong & Moskalenko 1998). However, inside GCs we have an additional component of optical photons which are emitted by stars of the cluster. Their spatial distribution is strongly non-uniform. It may reach a value about $w_{\text{op}}^0 = 300 \text{ eV cm}^{-3}$ for 47 Tuc and about $w_{\text{op}}^0 = 100 \text{ eV cm}^{-3}$ for Terzan 5 in the cluster center but decreases rapidly with the distance from the GC center. Thus, for 47 Tuc the spatial distribution of optical photons was derived by Michie (1963) and Kuranov & Postnov (2006), which is

$$w_{\text{op}}(r) = w_{\text{op}}^0 \times \begin{cases} 1, & \text{for } r < r_c \\ (r_c/r)^2, & \text{for } r_i > r > r_c \\ (r_c r_h)^2/r^4, & \text{for } r > r_i, \end{cases} \quad (6)$$

where $r_c = 0.5 \text{ pc}$, $r_i = 50 \text{ pc}$, and $r_h = \sqrt{2r_c r_i/3}$.

The diffusion coefficient inside clusters ($r < r_c$) is supposed to be smaller than in the surrounding medium, which seems to be reasonable, since GCs have high densities of stars with their winds which can create turbulence in the medium inside GCs. Therefore, the diffusion coefficient was taken in the form

$$D(r) = D_0 + D_1 \theta(r - r_D), \quad (7)$$

where $\theta(r)$ is the Heaviside (step) function. The values of D_0 and D_1 are derived from the data (see below). The value of $r_D = 100 \text{ pc} \simeq 2r_c$ is also derived from the spatial distribution of gamma-ray emission.

We assume that pulsars inject a monoenergetic spectrum of electrons in the form

$$Q(r, E) = \sum_n \frac{L_{\text{sd}}^n}{E_{\text{inj}}^n} \delta(E - E_{\text{inj}}^n) \delta(r - r_n), \quad (8)$$

where r_n is the position of the n th pulsar and the injection process is stationary. Here, L_{sd}^n is the spin-down loss rate of

the n th pulsar in the GC and the injection energy of electrons generated by each pulsar is estimated as (see Equation (3))

$$E_{\text{inj}} = 10^2 f_{e^\pm}^{-1} L_{34}^{1/2} \text{ GeV} = E_0 L_{34}^{1/2}, \quad (9)$$

where E_0 is a constant. In Section 3, we have pointed out that $f_{e^\pm} \sim 1$ for MSPs without outer gaps and $f_{e^\pm} \sim 30$ for MSPs with outer gaps, E_0 should be either $\sim 10^2 \text{ GeV}$ or $\sim 5 \text{ GeV}$. If the mean spin-down power of MSPs $L_{34} \sim 2$, then the possible range of E_{inj} should be 200 GeV for MSPs without outer gaps and 10 GeV with outer gaps.

For the source function Q , we estimate the cumulative contribution of all pulsars in the cluster. We estimate the required number of pulsars by matching the observed intensity of GeV gamma-ray emission from the clusters.

The process of IC scattering depends on the parameter $\xi = m_e c^2 / \epsilon \gamma$, where ϵ is the energy of a background photon and γ is the gamma-factor of electrons. If $\xi > 1$ then the scattering is classical and the total cross section of IC scattering equals the Thompson cross section, σ_T . In the case of $\xi < 1$, the cross section drops down as $\sigma \propto \sigma_T / \gamma$.

We note that the scattering of relativistic electrons on relic and on IR photons satisfies the condition $m_e c^2 > \epsilon \gamma$ and therefore is classical. For interactions of these electrons with optical photons, this condition may be violated. Then, the interaction of photon–electron is catastrophic when a significant part of the electron energy is transferred to a scattered photon. In this case, the exact Klein–Nishina cross section is used for calculations.

The scattered photon spectrum per electron is (see Blumenthal & Gould 1970)

$$\frac{d^2 N}{dt dE_1} = \frac{2\pi r_0^2 m c^3}{\gamma} \int \frac{n(\epsilon) d\epsilon}{\epsilon} \times \left[2q \ln q + (1 + 2q)(1 - q) + \frac{1}{2} \frac{(\Gamma q)^2}{1 + \Gamma q} (1 - q) \right], \quad (10)$$

where ϵ_1 is the energy of scattered photon, $E_1 = \epsilon_1 / \gamma m c^2$, $n(\epsilon)$ is the density of background photons, $\Gamma = 4\epsilon \gamma / m c^2$, and $q = E_1 / \Gamma(1 - E_1)$. The range of values of E_1 is restricted by the range

$$1 \gg \epsilon / \gamma m c^2 \geq E_1 \geq \Gamma / (1 + \Gamma). \quad (11)$$

The rates of electron energy losses in the two limit cases (the classical (Thompson) limit and the extreme Klein–Nishina limit) are

$$\left(\frac{dE}{dt} \right)_T = \frac{4}{3} \sigma_T c \gamma^2 w_{\text{em}} \left(\frac{dE}{dt} \right)_{\text{KN}} \\ = \pi r_0^2 m^2 c^5 \int \frac{n(\epsilon) d\epsilon}{\epsilon} \left(\ln \frac{4\epsilon \gamma}{m c^2} - \frac{11}{6} \right), \quad (12)$$

where w_{em} is the energy density of background photons.

To compare with observational data, we calculate the two parameters of IC gamma-ray flux from GCs. The first one is the flux of gamma-ray emission from the cluster

$$F(\epsilon_1) = \int dr \int dE f(r, E) \frac{1}{\gamma m c^2} \frac{d^2 N}{dt dE_1}, \quad (13)$$

where $f(r, E)$ is the solution of Equation (5).

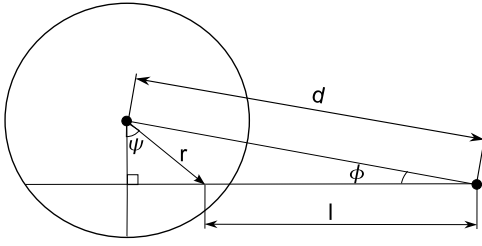


Figure 2. Schematic view of the cluster from Earth.

The second is the spatial distribution of the IC flux in the energy range $\Delta\epsilon$ as observed from Earth:

$$\Phi(\phi) = \int_{\Delta\epsilon} d\epsilon_1 \int f(r, \epsilon_1) dl(\phi). \quad (14)$$

Here, l is the line of sight and ϕ is the angular distance from the center as observed from Earth. The distance from the center of the cluster r can be estimated in the following way (see Figure 2):

$$r(l, \phi) = d \cdot \frac{\sin \phi}{\cos \psi}. \quad (15)$$

Equation (14) may be rewritten as

$$\Phi(\phi) = \int_{\Delta\epsilon} d\epsilon_1 \int_{-\pi/2}^{\pi/2-\phi} f(r, \epsilon_1) \frac{dl}{d\psi} d\psi, \quad (16)$$

where

$$\frac{dl}{d\psi} = d \cdot \frac{\sin \phi}{\cos^2 \psi}. \quad (17)$$

The energies of primary electrons, E , and scattered gamma-ray photons, ϵ_1 , are related to each other as

$$\epsilon_1 = \frac{4}{3} \epsilon \left(\frac{E}{mc^2} \right)^2 \quad (18)$$

in the classical limit and $\epsilon_1 \simeq E$ in the extreme Klein–Nishina limit.

The actual spin-down rate of individual MSPs in GCs is very difficult to determine due to the very strong gravitational force in the cores of GCs. Some attempts have been made to subtract the gravitational effect and recover the true spin-down rate of MSPs in GCs (e.g., Freire et al. 2001; Grindlay et al. 2002). In general, such a subtraction scheme is very reasonable; however it may not be correct for an individual pulsar. For example, the average gravitational field used is a simple function of distance from the center of the cluster to the pulsar. The observation can only determine the projected distance instead of the actual distance. Therefore, it is questionable whether the estimated spin-down rate for an individual pulsar is correct. On the other hand, this method may provide a good correction on average. In this paper, we assume for simplicity that each MSP in GC has the same spin-down power and we use the average spin-down power $\sim 2 \times 10^{34}$ erg s^{-1} estimated by Freire et al. (2001) and Grindlay et al. (2002) as the characteristic spin-down power of each MSP in our subsequent calculation. Then the total injection spectrum of electron/positron pairs produced by all pulsars of the cluster can be assumed as monoenergetic, $Q(E) \propto \delta(E - E_{inj})$, and the total number of electrons with energy E in the cluster is evaluated under the influence of IC/synchrotron losses that gives

$$\frac{dN_e}{dE_e} = f(E_e) \propto E_e^{-2} \theta(E_{inj} - E_e), \quad (19)$$

where E_{inj} is given by Equation (9).

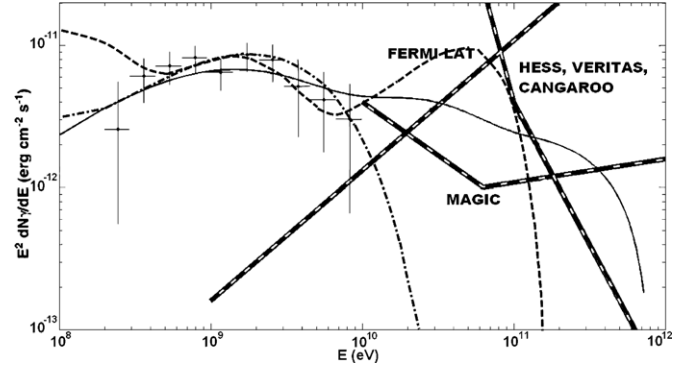


Figure 3. Gamma-ray flux from 47 Tuc obtained from the IC model. The data point from Abdo et al. (2009). The solid line corresponds to relic photon scattering, the dashed line corresponds to IR photon scattering, and the dash-dotted line corresponds to optical photon scattering. Sensitivities of different gamma-ray instruments are shown by the heavy dashed lines.

5. APPLICATIONS

5.1. 47 Tucanae

The flux of gamma rays expected in the IC model for the emission region within the diameter of 1° around the cluster center (Equation (13)) and the *Fermi* observational data are shown in Figure 3. We find that the optical photons emitted from the core of GC (see Equation (6)) do not contribute significantly in the gamma-ray flux produced by the IC scattering because their density decreases rapidly away from the core and the diffusion mean free path (see Equation (20)) is much larger than the size of the core. One can see from this figure that the data can be interpreted either by scattering on relic (solid line), IR (dashed line), or optical photons (dash-dotted line). The three peaks on each of these lines correspond to the scattering on relic, IR, and optical photons, respectively. Since the characteristic energies of soft photons from relic, IR, and optical components are different, to enable them to be scattered to the GeV range, one should use electrons with different energies in accordance with Equation (18). The energy parameter from Equation (9) corresponding to the relic scattering being responsible for the explanation of *Fermi* data is $E_{inj}^{relic} = 0.7$ TeV, to the IR scattering is $E_{inj}^{IR} = 0.15$ TeV, and to the optical scattering is $E_{inj}^{op} = 0.02$ TeV. As one can see from this figure, LAT, MAGIC, and even H.E.S.S. are able to detect the predicted excesses in the energy range above 10 GeV except the case when the GeV gamma-ray emission is produced by scattering on optical photons (the dash-dotted line). However, these excesses depend on the nature of the soft photons. In general, IR photons give the strongest excess in the 30 GeV range. If this flux level is detected, it supports that the GeV gamma rays have an IC origin. On the other hand, if the excess is found but is significantly weaker than the predicted level of the IC model, then part of the GeV gamma rays may still come from the CR mechanism as predicted by Venter et al. (2009). We also want to remark that although the upward scattered relic photons can fit the *Fermi* data, it requires E_{inj} larger than the estimated value by a factor of 3 (see discussion after Equation (9)), which is unfavorable unless the pair-creation process of MSPs in 47 Tuc is strongly suppressed.

The recent H.E.S.S. observations gave an upper limit $\sim 6.7 \times 10^{-13}$ cm $^{-2}$ s $^{-1}$ of gamma-ray photon flux for energies above 800 GeV (Aharonian et al. 2009) that is higher than we predict for 47 Tuc.

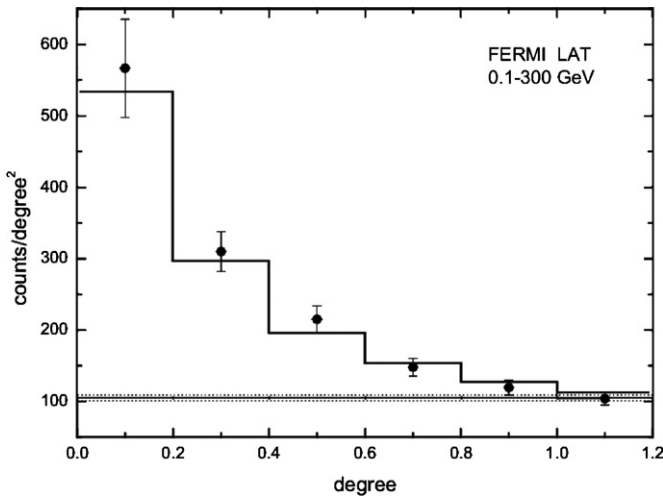


Figure 4. Spatial distribution of gamma-ray emission from the direction of 47 Tuc and the results of simulation.

We can compare the spatial distribution as expected from the IC model with the observed data. To obtain the γ -ray brightness profile of 47 Tuc, we have taken the LAT data obtained from 2008 August 4 to 2009 December 4. For the data filtering, we adopt the standard procedures suggested by the Fermi Science Support Center (for further details, please refer to Kong et al. 2010). We have binned the filtered event list into an image centered at the peak of the γ -ray emission with a bin size of 0.1 . The surface brightness profile of the γ rays from 47 Tuc is displayed in Figure 4. The average background level and its 1σ deviation are indicated by horizontal lines, which were calculated by sampling the source-free regions around 47 Tuc within a $10 \times 10 \text{ deg}^2$ field of view. The average background is estimated to have a level of $105 \pm 4 \text{ counts deg}^{-2}$. The observed data are nicely reproduced if the diffusion coefficients are the following (see Equation (7)): for relic scattering, $D_0^{\text{relic}} = 10^{27} \text{ cm}^2 \text{ s}^{-1}$, $D_1^{\text{relic}} = 5 \times 10^{27} \text{ cm}^2 \text{ s}^{-1}$; for IR scattering, $D_0^{\text{IR}} = 6 \times 10^{26} \text{ cm}^2 \text{ s}^{-1}$, $D_1^{\text{IR}} = 6 \times 10^{28} \text{ cm}^2 \text{ s}^{-1}$; for optical scattering, $D_0^{\text{op}} = 10^{26} \text{ cm}^2 \text{ s}^{-1}$, $D_1^{\text{op}} = 10^{27} \text{ cm}^2 \text{ s}^{-1}$. However, we want to emphasize that the contribution of unresolved point-like sources in the total gamma-ray flux of 47 Tuc observed by *Fermi* is unknown. If future observations show that this flux is really diffuse, it proves its IC origin. Here we have assumed that most point sources are located inside the cores of GCs and the angular resolution of future observations is good enough to remove the contribution from the core.

5.2. Terzan 5

The expected flux of gamma rays from Terzan 5 and the *Fermi* data are shown in Figure 5 by using the same set of diffusion coefficients as for 47 Tuc and the injected energy equals 180 GeV for IR photons and 25 GeV for optical photons. We find that it is impossible to use the relic photons to obtain reasonable fit to the *Fermi* data and the scattering on relic photons provides a negligible effect because of the very high density of IR and optical photons in Terzan 5. On the other hand, the IR or optical scattering can nicely reproduce the experimental data as shown in Figure 5.

As Terzan 5 is located in a more complicated environment than 47 Tuc, in particular it is located very close to the Galactic plane (see Figure 1 in Kong et al. 2010), this makes the estimation of its γ -ray brightness profile much more intricate. In

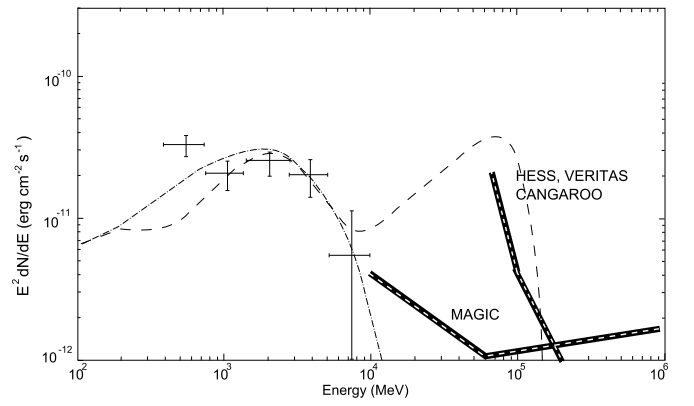


Figure 5. Gamma-ray flux from Terzan 5 obtained from the IC model. The dashed line corresponds to IR photon scattering and the dash-dotted line corresponds to optical photon scattering.

view of this difficulty, we do not compare the spatial distribution computed from the model with the observation for Terzan 5.

5.3. Model Fitting of Other Globular Clusters

We also apply our IC model to other clusters presented in the paper by Abdo et al. (2010b). The diffusion coefficients are the same as for 47 Tuc and Terzan 5 for simplicity. Although the Inverse Compton scattering (ICS) of the relic photons in some GCs may also fit the *Fermi* data, we have pointed out in Section 2.2 without another factor the MSP ratio between Terzan 5 and 47 Tuc required by the gamma-ray luminosity ratio is 12, which seems too large in comparing with the observed MSP ratio ~ 1.5 . Since the relic photon density is constant everywhere, it cannot reduce this ratio. Furthermore, they also cannot fit the *Fermi* data for Terzan 5 and the required E_{inj} is higher than the theoretical predicted value for 47 Tuc, therefore we conclude that the relic photons may not be the possible background soft photons to produce the gamma rays in the *Fermi* energy range. We will not use them in fitting the spectrum of the other six GCs in this subsection. However, the relic photons can still participate in the IC process and can contribute to X-rays significantly. In fitting these six new GCs, we vary slightly the parameter E_{inj} for different clusters. The values of E_{inj} as well as the effective output power ηL_{sd} , which is treated as a normalization factor in fitting, are presented in Table 1, and are fixed by comparing with the observed gamma-ray power of each cluster. The spectra of the clusters together with the data point from Abdo et al. (2010b) are presented in Figure 6. We can see that the IC model can fit the gamma-ray spectra of all eight GCs with similar parameters well (cf. Figure 6 and Table 1). In estimating the gamma-ray power from the GCs, we have used the observed energy fluxes and distances given in Abdo et al. (2010b).

5.4. Implications of the Fitting Parameters

In general, we need three parameters to fit the observed spectrum of GCs, i.e., diffusion coefficient, injected energy (E_{inj}), and η . Since we are fitting the total spectrum instead of the spatial dependent spectrum, the diffusion coefficient mainly controls the size of emission region, so for simplicity we have assumed that the diffusion coefficients of other GCs are the same as those of 47 Tuc. The exact value of the diffusion coefficient must be determined by measuring the angular size of the diffusion emission region. In the IC model, we predict that

Table 1
Fitting Parameters for IC Model for Eight Clusters from Abdo et al. (2010b)

Name	Infrared		Optical	
	E_{inj} (GeV)	ηL_{sd} (10^{34} erg s $^{-1}$)	E_{inj} (GeV)	ηL_{sd} (10^{34} erg s $^{-1}$)
M28	130	14.8	17	6.2
M62	180	21.8	25	10.9
NGC 6388	150	51.6	20	25.8
NGC 6440	150	47.5	20	19.0
NGC 6652	150	20.6	20	7.8
Omega Centauri	150	6.1	20	2.8
Terzan 5	180	49.1	25	25.7
47 Tuc	150	10.0	20	4.8

a very wide energy band will be produced (see the following section), therefore the angular size of other energy bands, e.g., radio and X-rays, can also be used to estimate the diffusion coefficient. The injected energy of pairs controls the spectral break and finally η , which can be interpreted as the efficiency for conversion of the spin-down power to the gamma-ray power times the total number of MSPs in the cluster and controls the magnitude of spectrum.

The injected energy given by Equation (9) depends on f_{e^\pm} (cf. Equation (2)). In Section 3, we discuss the possible values of f_{e^\pm} . If the outer gap exists in MSPs, $f_{e^\pm} \sim 30$, which gives $E_{\text{inj}} \sim 10$ GeV, which is less than the fitting values by a factor of 2 for optical photons. On the other hand, if pairs are only produced in the polar gap, we have estimated in Section 3 that $f_{e^\pm} \sim 1$, which gives $E_{\text{inj}} \sim 2 \times 10^2$ GeV. This estimate is consistent with the fitting values for IR as soft photons. However, if the optical photons are the soft photons, then this estimate is higher than the fitting values by a factor of 10 in general. This may imply that the outer gap exists but its pair production multiplicity is substantially lower than the previous model estimates, for example instead of closing the outer gap in terms of the photon–photon creation process the outer gap closed by magnetic pair creation is possible (cf. Takata et al. 2010), which gives less outgoing pairs. However, if this is the case, CR contribution cannot be avoided. The observed gamma rays in the *Fermi* energy range should be a mixture of the CR and IC processes.

In fitting data point of view, ηL_{sd} is the normalization factor. In our model, it can be estimated by relating the observed gamma-ray power L_γ to the theoretical IC power, i.e., $N_{\text{MSP}} L_{e^\pm}$, where N_{MSP} is the total number of MSPs in the GC and L_{e^\pm} is the part of spin-down power carried away by the pairs given by Equation (4). If we assume that each pulsar has a similar spin-down power, e.g., $L_{34} \sim 2$, once f_{e^\pm} is fixed, then we can use the above conservation to estimate the total number of MSPs in the GC. Let us assume that the outer gap does not exist, we have estimated in Section 3 that the fraction of spin-down power carried away by pairs is about 0.1. Using Table 1 and assuming IR as the IC soft photons, we can estimate that the number of MSPs for 47 Tuc and Terzan 5 are ~ 50 and ~ 245 , respectively.

6. MODEL CONSTRAINTS BY OTHER ENERGY BANDS

Although the IC scattering can explain the *Fermi* data of both clusters very well, we cannot distinguish from the data scattering on which photons, i.e., optical, IR, and relic, produce this gamma-ray flux. For 47 Tuc, all three cases are equally possible. For Terzan 5, the scattering on galactic infrared photons and

optical photons can be possible candidates. In this section, we will explore the constraints for the model derived from other energy bands.

The IC scattering cooling time is given by $\tau_{\text{cooling}} \sim 4 \times 10^{14} \gamma_{w5}^{-1} w_{-12}^{-1} \text{s}$, where γ_{w5} is the Lorentz factor of the relativistic electron/positron pairs in units of 10^5 and w_{-12} is the energy density of soft photon in units of $10^{-12} \text{erg cm}^{-3}$. The diffusion time of these pairs over the distance d is given by $\tau_d \sim 10^{11} d^2 D_{26}^{-1} \text{s}$, where d is in units of pc and D_{26} is the diffusion coefficient in units of $10^{26} \text{cm}^2 \text{s}^{-1}$. Therefore, the diffusion radius is estimated from the equality $\tau_{\text{cooling}} = \tau_d$ and is given by

$$d \approx 63 \gamma_{w5}^{-1/2} w_{-12}^{-1/2} D_{26}^{1/2} \text{pc}. \quad (20)$$

Since the total IC photon spectrum from the GC is given by

$$\Phi(\epsilon_\gamma) = \int_{E_e} n_{\text{ph}}(\epsilon_{\text{ph}}) c \frac{dN}{dE_e} \frac{d\sigma_{\text{IC}}}{d\epsilon_\gamma} dE_e, \quad (21)$$

where $\frac{dN}{dE_e}$ is given by Equation (19), the photon spectral index is ~ -1.5 (see Blumenthal & Gould 1970). Here, $d\sigma_{\text{IC}}/d\epsilon_\gamma$ is the IC differential cross section which in the classical limit is approximately

$$\frac{d\sigma_{\text{IC}}}{d\epsilon_\gamma} = \sigma_T \delta \left(\epsilon_\gamma - \frac{4}{3} \epsilon_{\text{ph}} \left(\frac{E_e}{mc^2} \right)^2 \right). \quad (22)$$

The energies ϵ_{ph} and ϵ_γ are the energies of background and scattered photons, respectively, and n_{ph} is the photon density of background photons.

The power in IC X-ray emission with the energy ϵ_x can be produced by scattering on different background photons. As compared with the contribution from scattering on the relic photons, we have

$$\frac{\Phi(\epsilon_x)_{\text{relic}}}{\Phi(\epsilon_x)_{\text{ph}}} \simeq \frac{w_{\text{relic}}}{w_{\text{ph}}} \sqrt{\frac{\epsilon_{\text{ph}}}{\epsilon_{\text{relic}}}}, \quad (23)$$

where ϵ_{relic} and ϵ_{ph} are the energies of relic and any other sort of background photons, respectively, and w is the corresponding energy density of photons. Equation (23) can be directly obtained by integrating Equation (21) subject to the constraint of the δ -function of Equation (22), i.e., after integration using $E_e = mc^2(\epsilon_x/\epsilon_{\text{ph}})^{1/2}$ to replace E_e , and $w_{\text{ph}} = \epsilon_{\text{ph}} n_{\text{ph}}$. In Figure 1, we can see that for 47 Tuc the energy densities of different soft photons are very closed, therefore the IC X-ray emission is mainly contributed from the IC scattering

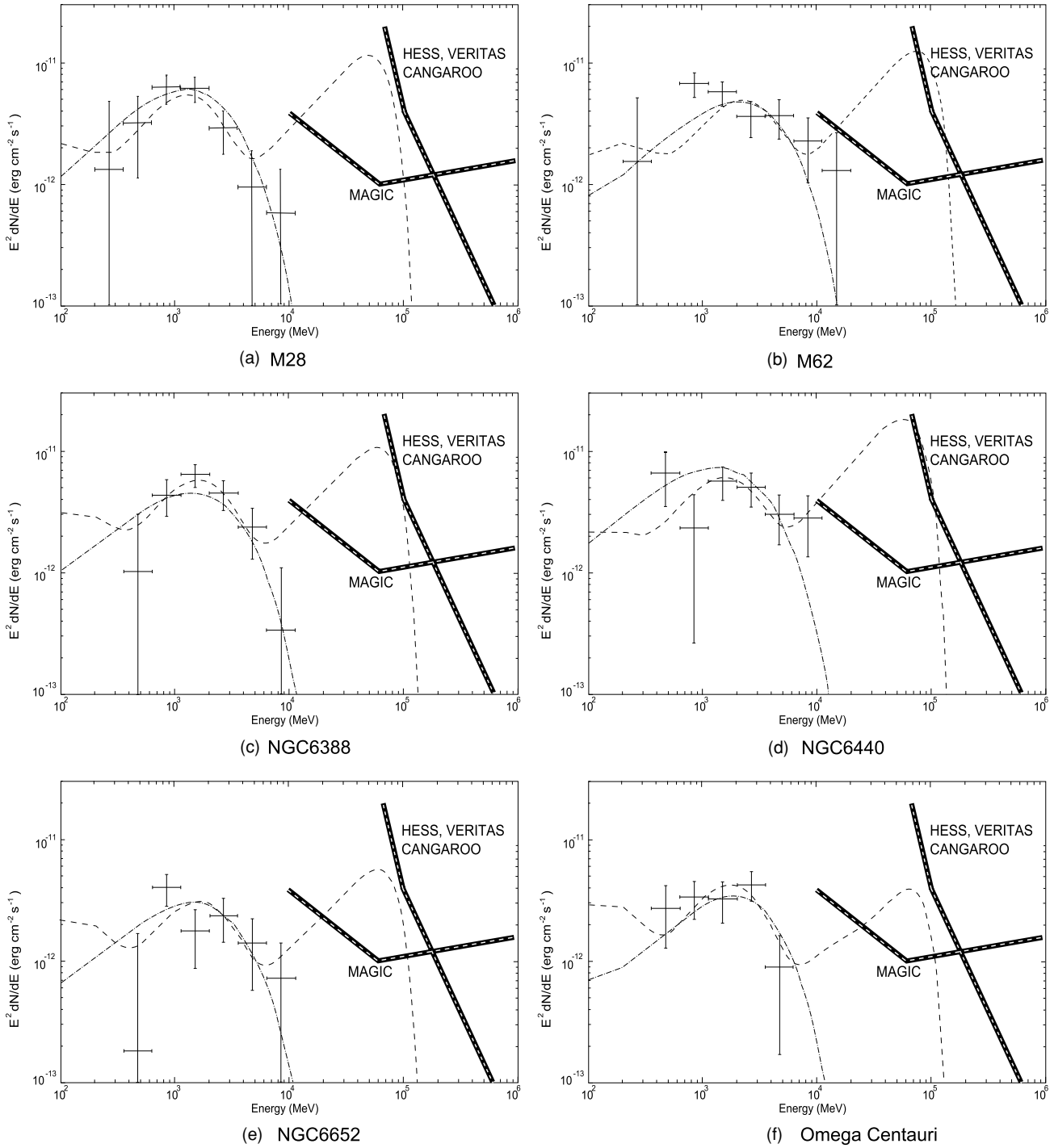


Figure 6. Experimental data for six GCs by Abdo et al. (2010b) along with IC model data for IR photons scattering (dashed line) and optical photons scattering (dash-dotted line).

of relic photons. For Terzan 5, although the ratios of the energy density between the IR photons and the relic photons, and between the optical photons and the relic photons are ~ 4 and ~ 40 , respectively, $\sqrt{\frac{\epsilon_{\text{IR}}}{\epsilon_{\text{relic}}}}$ and $\sqrt{\frac{\epsilon_{\text{optical}}}{\epsilon_{\text{relic}}}}$ are close to ~ 4 and ~ 40 , respectively. Therefore, the contributions to IC X-rays by the relic photons, IR, and optical photons are comparable. However, it is very important to note that although the energy flux of IC X-rays from each of these three soft photons is comparable, they are emitted from different regions. For example, most of the IC X-rays by scattering relic photons come from a few arcmins

region, whereas IC X-rays by scattering IR photons and optical photons come from a much bigger radius because the electrons/positrons are cooling off on the way diffusing out from the core.

The X-ray energy flux at 5 keV ($F(\epsilon_\gamma = 5 \text{ keV})$) can be estimated as follows. Since IC energy flux is given by $F(\epsilon_\gamma) \approx \epsilon_\gamma^2 \Phi(\epsilon_\gamma) \sim \epsilon_\gamma^{1/2}$ because $\frac{dN}{dE_e} \sim E_e^{-2}$, we can estimate the energy flux at 5 keV $F(\epsilon_\gamma = 5 \text{ keV})$ from its peak energy flux. We have argued that the relic photons should be the most important photons to generate the X-rays through the IC process, therefore $F(\epsilon_\gamma = 5 \text{ keV})$ produced by the IC of relic photons is

given by

$$F_x(5 \text{ keV}) \approx (5 \text{ keV}/8\gamma_{w5}^2 \text{ MeV})^{1/2} F_{\text{relic}}, \quad (24)$$

where F_{relic} is the peak energy flux of the IC scattering relic photons and the characteristic upward scattering energy of relic photons is $\sim 8\gamma_{w5}^2 \text{ MeV}$. We can estimate the peak energy flux of the scattered relic photons by $F_{\text{relic}} = (w_{\text{relic}}/w_{\text{soft}})F_{\gamma}^{\text{obs}}$, where F_{γ}^{obs} is the observed gamma-ray energy flux in the GeV energy range, w_{relic} and w_{soft} are the energy density of the relic photons and the soft photons, respectively, which upward scatter to produce gamma rays.

The strength of the magnetic field B near the clusters is not known exactly, it is estimated to be of the order of 10^{-6} G (Beck et al. 2003). The energy loss ratio between synchrotron radiation and IC scattering is given by

$$F_{\text{syn}} \approx F_{\gamma} \frac{B^2/8\pi}{w_{\text{soft}}} = 3 \times 10^{-2} B_{-6}^2 (w_{-12}^{\text{soft}})^{-1} F_{\gamma}, \quad (25)$$

where B_{-6} is the magnetic field in units of 10^{-6} G . We can see that the synchrotron loss is not negligible. The characteristic synchrotron frequency is given by

$$\nu_{\text{syn}} = \gamma_w^2 \frac{eB}{2\pi mc} = 4.4 \times 10^{10} \gamma_{w5}^2 B_{-6} \text{ Hz}, \quad (26)$$

which is in the radio band. We can estimate the energy flux at 1 GHz

$$F_{1 \text{ GHz}} \approx (1 \text{ GHz}/\nu_{\text{syn}})^{0.5} F_{\text{syn}} \quad (27)$$

if $\nu_{\text{syn}} > 1 \text{ GHz}$. $F(\nu)$ corresponds to energy flux but it is more useful to estimate the differential flux per Hz measured in Jy. To obtain it, one can divide the energy flux by characteristic frequency.

6.1. 47 Tuc

We have pointed out that the angular resolution of *Fermi* is of the order of $\sim 1^\circ$ and the angular resolution of H.E.S.S. is also of the order of $\sim 1^\circ$. This angular size implies that the emission radius of 47 Tuc is $\leq 80 \text{ pc}$. In fitting the gamma-ray spectrum, we find that basically we cannot differentiate which kind of soft photons produces the observed gamma rays. However, from Equation (24), the predicted X-ray energy flux depends on the Lorentz factors, which are $\gamma_w = 1.4 \times 10^6$ for relic photons, $\gamma_w = 2.8 \times 10^5$ for IR photons, and $\gamma_w = 4 \times 10^4$ for optical photons. The predicted X-ray energy fluxes are $F_x(5 \text{ keV}) \approx (5 \text{ keV}/8\gamma_{w5}^2 \text{ MeV})^{0.5} (w_{\text{relic}}/w_{\text{soft}}) F_{\gamma} \sim 1.8 \times 10^{-14} \text{ erg cm}^{-2} \text{ s}^{-1}$ for relic photons, $\sim 10^{-13} \text{ erg cm}^{-2} \text{ s}^{-1}$ for IR photons, and $\sim 3.2 \times 10^{-13} \text{ erg cm}^{-2} \text{ s}^{-1}$ for optical photons, respectively, in 1° radius.

With the *Chandra* observation, Okada et al. (2007) have reported two extended X-ray features potentially associated with 47 Tuc which are labeled as T1 and T2 in their Figure 1(a). However, a recent deep *Suzaku* observation reported by Yuasa et al. (2009) found that the X-ray spectrum T1 is consistent with a redshifted thermal plasma and suggest its nature as a background galaxy cluster. On the other hand, T2 is relatively fainter and locates just outside the half-mass radius of 47 Tuc. Its spectrum can be modeled by a power law with a photon index of $\Gamma \sim 2.2$. The flux of this feature is found to be $\sim 7 \times 10^{-14} \text{ erg cm}^{-2} \text{ s}^{-1}$. Although the interpretation that this feature arises via ICS is tempting (see also Krockenberger

& Grindlay 1995), it should be noted that it locates very close to the very bright emission of T1. Also, both features locate at a large off-axis angle in this *Chandra* observation which result in a rather wide point-spread function at their locations. Therefore, at least a fraction of the X-rays from T2 can possibly be contributed by T1. Furthermore, the tidal radius of 47 Tuc is $43'$ and it is possible that a good fraction of MSPs are located outside the half-mass radius but within the tidal radius. Consequently, the center of this extended faint X-ray source T2 may not coincide with the half-mass radius. With this consideration, the flux measured from T2 should be considered as an upper limit. The largest model-predicted X-ray energy flux in $3'$ radius resulting from optical photons is $\sim (3'/1^\circ)^2 3.2 \times 10^{-13} \text{ erg cm}^{-2} \text{ s}^{-1} \sim 10^{-15} \text{ erg cm}^{-2} \text{ s}^{-1}$. However, it is very important to note that the actual emission region of gamma rays can be much smaller than 1° as this estimate is limited by the angular resolution of LAT. Therefore, a dedicated X-ray observation with T2 on-axis can provide an important constraint for the model parameters.

According to Equation (27), the energy fluxes at 1 GHz are $9 \times 10^{-14} \text{ erg cm}^{-2} \text{ s}^{-1}$ for optical photons, $5 \times 10^{-14} \text{ erg cm}^{-2} \text{ s}^{-1}$ for IR photons, and $5 \times 10^{-15} \text{ erg cm}^{-2} \text{ s}^{-1}$ for relic photons in 1° , which correspond to 9 Jy, 5 Jy, and 0.5 Jy, respectively. At 400 MHz, the corresponding fluxes will be equal to 18 Jy, 8 Jy, and 0.7 Jy.

The radio flux from the region with diameter 1° is 19 Jy at 408 MHz (Haslam et al. 1982) and 27 Jy at 1420 MHz (Reich et al. 2001). However, in view of the poor resolution of the instrument, there may have been contamination by other sources. Therefore, the true radio fluxes due to the pulsar wind at these frequencies should be lower than the aforementioned values. In view of this, these observed values should only be considered as the upper limits. Since the theoretical estimate at 400 MHz for the background optical photons (i.e., 18 Jy) is comparable with the observational limit reported by Haslam et al. (1982), there is a high probability that the IC model with the optical photons as the soft photon field may overpredict the radio flux. In Section 5.4, we have pointed out that the injected energy E_{inj} for optical photons is less than the model-predicted value by a factor of ~ 10 if the outer gap does not exist (cf. Equation (9) and Table 1). If the outer gap indeed exists in MSPs of GCs, the CR must contribute to GeV gamma rays and hence the contribution by the IC component is only partial. The predicted diffuse radio flux for the background optical photons above assumed that all observed GeV gamma rays result from IC. If this is not the case then the reduction of the diffuse radio flux should be pro rata. On the other hand, for the other soft photon fields (i.e., IR and relic photons), the IC model-predicted flux densities appear to be more consistent with this limit. At 1 GHz, the IC model-predicted values for all the soft photon fields in our consideration are far below the observed upper bound at 1.4 GHz (Reich et al. 2001). This suggests that the currently available observational results do not allow us to put a tight constraint at this frequency. Future radio observations with higher resolution and sensitivity can possibly help us to discriminate different scenarios. Since the radio flux and gamma-ray flux are correlated, more detailed observations in the radio band may provide better constraint on these models.

6.2. Terzan 5

Chandra has also detected diffuse X-ray emission in the 2–7 keV band from Terzan 5 (Eger et al. 2010) and the X-ray energy flux is $5 \times 10^{-13} \text{ erg cm}^{-2} \text{ s}^{-1}$. Unlike in the case of

47 Tuc, whose diffuse X-ray is most likely from the unresolved X-ray point sources as suggested by Okada (2005), some diffuse X-ray emission in Terzan 5 clearly exists from $90''$ to $160''$ even if an unresolved point source is subtracted. In other words, the X-ray emission region is ~ 10 pc. If the diffuse X-ray is the tail of the IC scattering, we can use it to constrain the theoretical models. In fitting the gamma-ray spectrum of Terzan 5, upward scattering either the galactic infrared photons or the optical photons is possible. However, the required Lorentz factors for IR and optical are 2.8×10^5 and 4×10^4 , and the energy densities are $\sim 10^{-12}$ erg cm $^{-3}$ and $\sim 6 \times 10^{-12}$ erg cm $^{-3}$, respectively. If the emission region is really 10 pc, then the diffusion coefficient of Terzan 5 is much smaller than that of 47 Tuc. According to Equation (20), it gives $D \sim 10^{25}$ cm 2 s $^{-1}$. The locations of 47 Tuc and Terzan 5 are very different, the former is above the galactic plane and the latter is in the galactic plane. This factor may cause the difference in the diffusion coefficient. According to Figure 1, $\epsilon_{\text{relic}}/\epsilon_{\text{IR}} \sim 0.3$ and $\epsilon_{\text{relic}}/\epsilon_{\text{optical}} \sim 0.05$, by using Equation (24) the predicted X-ray energy fluxes are $\sim 7 \times 10^{-14}$ erg cm $^{-2}$ s $^{-1}$ and $\sim 10^{-13}$ erg cm $^{-2}$ s $^{-1}$, respectively. These predicted values are about a factor of 3–4 lower than that of the observed value. However, in Figure 2 of Eger et al. (2010), we can see that if the unresolved X-ray point source can contribute to the diffuse X-ray, then after subtracting this contribution (the green solid curve) the real diffuse X-ray flux is actually reduced significantly.

Again, we can use Equation (27) to estimate the predicted radio energy flux, which gives $\sim 5 \times 10^{-14}$ erg cm $^{-2}$ s $^{-1}$ for the IR model and $\sim 3.4 \times 10^{-14}$ erg cm $^{-2}$ s $^{-1}$ for the optical model (5 Jy and 3.4 Jy). We do not have radio data for the $3'$ region around Terzan 5. If observations show the lower values of radio flux from the corresponding region, then radio emission, gamma-ray emission, and X-ray emission should occupy a more extended region. In that case, the observed diffuse X-ray emission from the $3'$ region should not be related to the IC model and should have a different nature. More detailed observations including spatial and spectral information by *Fermi* and other higher energy detectors, such as H.E.S.S., MAGIC, VERITAS, etc., as well as radio observations can provide better constraints for the models.

7. DISCUSSION

We have calculated the GeV gamma-ray spectrum produced by IC scattering between the relativistic e^\pm pairs of the pulsar wind and the background soft photons, which include the relic photons, the star lights of the cluster, the infrared photons, and the star-light photons from the Galactic disk. We obtain the steady-state spatial and energy distribution function of e^\pm pairs by solving the standard diffusion equation for describing the cosmic-ray propagation in the interstellar medium. We find that most of the high-energy radiation comes from a region outside the core of GCs with a radius > 10 pc. In fact, the contribution by upward scattering the star-light photons inside the cluster core region is negligible in contradiction to the previous calculations (e.g., Bednarek & Sitarek 2007). For 47 Tuc, the GeV photons detected by *Fermi* can be reproduced by the upward scattering of all three possible background soft photon fields, i.e., relic photons, IR photons, and optical photons. There is no compelling evidence to rule out any of these three models, but the required energy of electrons/positrons for Compton upscattering the relic photons to the GeV energy range is a factor of 3 higher than that predicted by the model. For Terzan 5, both the galactic IR and optical photons

are possible soft photons for upward scattering to produce the GeV gamma rays. Again, there is no compelling evidence to differentiate these two models. Obviously, the optical one cannot produce photons higher than 10 GeV.

It is generally agreed that gamma-ray emissions from GCs are associated with MSPs inside the clusters. It has been standard to explain the spectra of almost all *Fermi*-LAT pulsars including MSPs, except very young Crab-like pulsars, in terms of the CR mechanism, i.e., gamma rays are emitted from inside the light cylinder. In this paper, we propose an alternative model, which fits the GeV spectra of all eight *Fermi*-detected GCs very well. The IC model predicts that: (1) the 100 MeV–100 GeV spectrum is correlated and hence some GCs should be sources for MAGIC and H.E.S.S. (2) Although IC is the main energy dissipation process, the synchrotron radiation cannot be avoided and results in diffuse radio emission. This prediction can best be tested by SKA, which has both excellent sensitivity and spatial resolution. (3) The gamma-ray power from GCs not only depends on the number of MSPs but also on the galactic soft photon density at the location of GCs, which is also a test between the CR model and the IC model. However, even though all these predictions are correct, this cannot rule out the CR model because it is possible that some fraction of the observed gamma-ray photons are a mixture of two origins. Actually, it is better to subtract the contribution from the CR model from the data and then compare with the model predictions of the IC model. However, it is practically impossible to carry out such an analysis because in order to calculate the CR spectrum from pulsars accurately the period and magnetic field of each pulsar must be known. Most MSPs in GCs have not been found even for 47 Tuc and Terzan 5. The contributions from these undetected MSPs are extremely difficult to estimate. In fact, Omega Centauri does not have any reported MSPs. This makes such a subtraction scheme impossible. Therefore, it is more important to prove the predictions of the IC model, such as the diffuse emission in various other energy bands, i.e., radio, X-rays, and very high energy (VHE). In future, we can use these data to constrain the relative contributions between these two different models.

Finally, we want to remark that by using the eight GCs reported by Abdo et al. (2010b) and seven newly confirmed gamma-ray GCs by Tam et al. (2010), Hui et al. (2010b) have carried out a correlation analysis between the observed γ -ray luminosities L_γ and various cluster properties to probe the origin of the high-energy photons from these GCs. They find that L_γ is positively correlated with the encounter rate Γ_c and the metallicity [Fe/H], which is an alternative independent estimator for the number of MSPs in the GCs (cf. Hui et al. 2010a). They also find a tendency that L_γ increases with the energy densities of the soft photon at the cluster location which favors the scenario that the observed gamma rays from these GCs are significantly contributed by the IC scattering. It should be noted that Hui et al. (2010b) have used different ways to calculate the encounter rate in comparing with Abdo et al. (2010b). Hui et al. (2010b) have included the observed dispersion velocity in evaluating Γ_c , whereas Abdo et al. (2010b) have used the free-fall velocity to approximate the dispersion velocity. For illustration purposes in Figure 7 we follow the definition of encounter rate given in Abdo et al. (2010b). Figure 7(a) shows the correlation between the gamma-ray luminosity and the encounter rate, and the correlation coefficient is 0.71. Figures 7(b) and (c) show strong correlations between L_γ and the combined factor, i.e., $\Gamma_c w_{\text{ph}}$, where w_{ph}

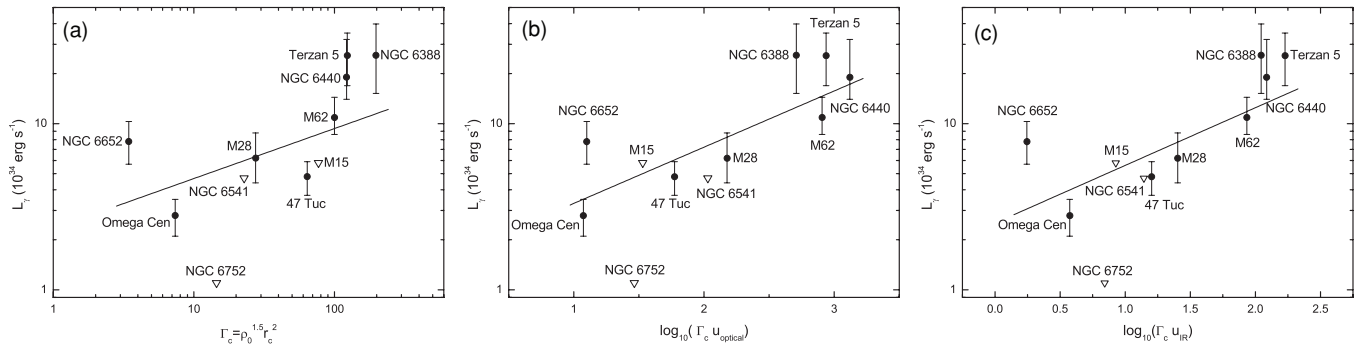


Figure 7. (a) Correlation between L_γ vs. Γ_c , (b) L_γ vs. $\Gamma_c w_{\text{IR}}$, and (c) L_γ vs. $\Gamma_c w_{\text{opt}}$. Data obtained from Abdo et al. (2010b).

are optical and IR photon energy density, respectively. The correlation coefficients for Figures 7(b) and (c) are 0.79 and 0.82, respectively, which show stronger correlations when the soft photon energy density is included. These results support that the IC scattering mechanism is at least one of the major gamma-ray emission processes in GCs.

K.S.C. is supported by a GRF grant of Hong Kong Government under HKU700908P, D.O.C. and V.A.D. are partly supported by the RFBR grant 08-02-00170-a, the NSC-RFBR Joint Research Project RP09N04 and 09-02-92000-HHC-a and by the grant of a President of the Russian Federation “Scientific School of Academician V. L. Ginzburg,” and A.K.H.K. is partly supported by the National Science Council of the Republic of China (Taiwan) through grant NSC96-2112-M007-037-MY3.

REFERENCES

- Abdo, A. A., et al. 2009, *Science*, **325**, 848
 Abdo, A. A., et al. 2010a, *ApJS*, **188**, 405
 Abdo, A. A., et al. 2010b, arXiv:1003.3588v1
 Aharonian, F., et al. 2009, *A&A*, **499**, 273
 Alpar, M. A., Cheng, A. F., Ruderman, M. A., & Shaham, J. 1982, *Nature*, **300**, 728
 Beck, R., Shukurov, A., Sokoloff, D., & Wielebinski, R. 2003, *A&A*, **411**, 99
 Bednarek, W., & Sitarek, J. 2007, *MNRAS*, **377**, 920
 Berezhinskii, V. S., Bulanov, S. V., Dogiel, V. A., Ginzburg, V. L., & Ptuskin, V. S. 1990, in *Astrophysics of Cosmic Rays*, ed. V. L. Ginzburg (North-Holland: Amsterdam)
 Blumenthal, G. R., & Gould, R. J. 1970, *Rev. Mod. Phys.*, **42**, 237
 Bogdanov, S., Grindlay, J. E., Heinke, C. O., Camilo, F., Freire, P. C., & Becker, W. 2006, *ApJ*, **646**, 1104
 Camilo, F., Lorimer, D. R., & Freire, P. 2000, *ApJ*, **535**, 975
 Camilo, F., & Rasio, F. A. 2005, in *ASP Conf. Ser. 328, Binary Radio Pulsars*, ed. F. A. Rasio & I. H. Stairs (San Francisco, CA: ASP), 147
 Cheng, K. S., Ho, C., & Ruderman, M. 1986, *ApJ*, **300**, 500
 Cheng, K. S., & Taam, R. E. 2003, *ApJ*, **598**, 1207
 Cheng, K. S., Taam, R. E., & Wang, W. 2004, *ApJ*, **617**, 480
 Cheng, K. S., Taam, R. E., & Wang, W. 2006, *ApJ*, **641**, 427
 Cheng, K. S., & Zhang, L. 1999, *ApJ*, **515**, 337
 Chevalier, R. A. 2000, *ApJ*, **539**, L45
 Clark, G. W. 1975, *ApJ*, **199**, L143
 Coroniti, F. V. 1990, *ApJ*, **349**, 538
 Dyks, J., & Rudak, B. 2000, *A&A*, **360**, 263
 Eger, P., Domainko, W., & Clapson, A.-C. 2010, *A&A*, **513**, A66
 Fawley, W. M., Arons, J., & Scharlemann, E. T. 1977, *ApJ*, **217**, 227
 Freire, P. C., Camilo, F., Lorimer, D. R., Lyne, A. G., Manchester, R. N., & D’Amico, N. 2001, *MNRAS*, **326**, 901
 Fruchter, A. S., & Goss, W. M. 1990, *ApJ*, **365**, L63
 Fruchter, A. S., & Goss, W. M. 2000, *ApJ*, **536**, 865
 Goldreich, P., & Julian, W. H. 1969, *ApJ*, **157**, 869
 Grindlay, J. E., Camilo, F., Heinke, C. O., Edmonds, P. D., Cohn, H., & Luger, P. 2002, *ApJ*, **581**, 470
 Harding, A. K., Usov, V. V., & Muslimov, A. G. 2005, *ApJ*, **622**, 531
 Haslam, C. G. T., Salter, C. J., Stoffel, H., & Wilson, W. E. 1982, *A&AS*, **47**, 1
 Heinke, C. O., et al. 2005, *ApJ*, **625**, 796
 Hessels, J. W. T., Ransom, S. M., Stairs, I. H., Freire, P. C. C., Kaspi, V. M., & Camilo, F. 2006, *Science*, **311**, 1901
 Hui, C. Y., & Becker, W. 2006, *A&A*, **448**, L13
 Hui, C. Y., Cheng, K. S., & Taam, R. E. 2009a, *ApJ*, **700**, 1233
 Hui, C. Y., Cheng, K. S., & Taam, R. E. 2010a, *ApJ*, **714**, 1149
 Hui, C. Y., Cheng, K. S., Wang, Y., Tam, P. H. T., Kong, A. K. H., Chernyshov, D. O., & Dogiel, V. A. 2010b, *ApJ*, submitted
 Hui, C. Y., Huang, H. H., Cheng, K. S., Taam, R. E., & Becker, W. 2009b, in *ASP Conf. Ser. 404, The Eighth Pacific Rim Conference on Stellar Astrophysics: A Tribute to Kam-Ching Leung*, ed. B. Soonthornthum et al. (San Francisco, CA: ASP), 149
 Ivanova, N. 2006, *ApJ*, **636**, 979
 Katz, J. I. 1975, *Nature*, **253**, 698
 Kennel, C. F., & Coroniti, F. V. 1984, *ApJ*, **283**, 694
 Kong, A. K. H., Hui, C. Y., & Cheng, K. S. 2010, *ApJ*, **712**, L36
 Krockenberger, M., & Grindlay, J. E. 1995, *ApJ*, **451**, 200
 Kuranov, A. G., & Postnov, K. A. 2006, *Astron. Lett.*, **32**, 393
 Michie, R. W. 1963, *MNRAS*, **125**, 127
 Okada, Y. 2005, PhD thesis, Tokyo Univ.
 Okada, Y., Kokubun, M., Yuasa, T., & Makishima, K. 2007, *PASJ*, **59**, 727
 Ransom, S. M., Hessels, J. W. T., Stairs, I. H., Freire, P. C. C., Camilo, F., Kaspi, V. M., & Kaplan, D. L. 2005, *Science*, **307**, 892
 Rees, M. J., & Gunn, J. E. 1974, *MNRAS*, **167**, 1
 Reich, P., Testori, J. C., & Reich, W. 2001, *A&A*, **376**, 861
 Ruderman, M. 1991, *ApJ*, **366**, 261
 Ruderman, M., & Cheng, K. S. 1988, *ApJ*, **335**, 306
 Ruderman, M., & Sutherland, P. 1975, *ApJ*, **196**, 51
 Spergel, D. N. 1991, *Nature*, **352**, 221
 Stappers, B. W., Gaensler, B. M., Kaspi, V. M., van der Klis, M., & Lewin, W. H. G. 2003, *Science*, **299**, 1372
 Strong, A. W., & Moskalenko, I. V. 1998, *ApJ*, **509**, 212
 Takata, J., Wang, Y., & Cheng, K. S. 2010, *ApJ*, **715**, 1318
 Tam, P. H., Kong, A. K. H., Hui, C. Y., & Cheng, K. S. 2010, *ApJ*, submitted
 Venter, C., & de Jager, O. C. 2008, *ApJ*, **680**, L125
 Venter, C., de Jager, O. C., & Clapson, A.-C. 2009, *ApJ*, **696**, L52
 Verbunt, F., & Hut, P. 1987, in *IAU Symp. 125, The Origin and Evolution of Neutron Stars*, ed. D. J. Helfand & J.-H. Huang (Dordrecht: Reidel), 187
 Verbunt, F., Lewin, W. H. G., & van Paradijs, J. 1989, *MNRAS*, **241**, 51
 Wang, W., Jiang, Z. J., & Cheng, K. S. 2005, *MNRAS*, **358**, 263
 Wang, W., Pun, C. S. J., & Cheng, K. S. 2006, *A&A*, **446**, 943
 Yuasa, T., Nakazawa, K., & Makishima, K. 2009, *PASJ*, **61**, 1107
 Zavlín, V. E. 2006, *ApJ*, **638**, 951
 Zhang, L., & Cheng, K. S. 1997, *ApJ*, **487**, 370
 Zhang, L., & Cheng, K. S. 2003, *A&A*, **398**, 639